Journal of Thermal Analysis and Calorimetry, Vol. 94 (2008) 2, 361–365

THERMAL BEHAVIOR OF MANNICH BASE N,N'-TETRA(4-ANTIPYRYL-METHYL)-1,2-DIAMINOETHANE (TAMEN) AND ITS COMPLEXES
Part II. The binuclear Cu(II) and Co(II) complexes

Elena Maria Mosoarca[*], *Sasca Viorel, Livia Avram, Ramona Tudose and Otilia Costisor*

Institute of Chemistry, Timişoara of Romanian Academy, 24 Mihai Viteazu Bd., 300223, Timişoara, Romania

The thermal decomposition in air and in nitrogen atmosphere of binuclear complex compounds of Cu(II) and Co(II) containing the Mannich base N,N'-tetra(4-antipyrylmethyl)-1,2 diaminoethane (TAMEN) as a ligand, $Cu_2(TAMEN)Cl_4$ and $Co_2(TAMEN)Cl_4$, were investigated. X-ray powder diffractometry, infrared spectroscopy and simultaneous thermogravimetry-differential thermal analysis (TG-DTA), have been used to characterize and to study the thermal behavior of these compounds. The results provided information concerning the stoichiometry, crystallinity, thermal stability and decomposition mechanism of the compounds.

Keywords: *binuclear complex, cobalt(II), copper(II), Mannich base, pyrazolone, thermal behavior*

Introduction

A series of cobalt(II) and copper(II) complexes containing antipyrine derivatives as ligands have been synthesized and some of them have been thermal or/and biological investigated [1–16]. In the first part of our work we have investigated the thermal behavior of Mannich base N,N'-tetra(4-antipyrylmethyl)-1,2-diaminoethane (TAMEN) and its Ni(II) complex, $Ni_2(TAMEN)Cl_4$ [17]. The synthesis and physico-chemical characterisation were presented in previous paper [6]. In this paper, the binuclear complex compounds containing Cu(II) and Co(II) cations and N,N'-tetra(4-antipyrylmethyl)-1,2-diaminoethane (TAMEN) as ligand, were investigated by means of simultaneous TG-DTA and complementary technique, X-ray powder diffractometry, infrared spectroscopy were used in order to observe the decomposition stages. The results of the present study improve the knowledge on these compounds including their thermal stability and reaction mechanism of decomposition process.

Results and discussion

Thermoanalytical studies of binuclear complexes

The thermal decomposition curves for the $Cu_2(TAMEN)Cl_4{\cdot}3H_2O$ in air and nitrogen dynamic atmosphere can be seen in Figs 1 and 2.

The thermal decomposition data for $Cu_2(TAMEN)Cl_4{\cdot}3H_2O$ are given in Table 1.

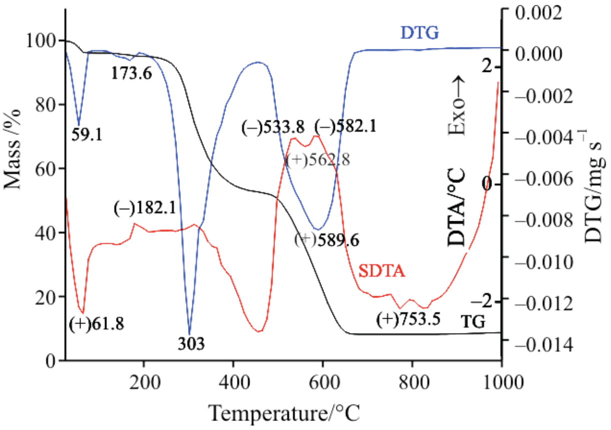

Fig. 1 The thermal decomposition curves of $Cu_2(TAMEN)Cl_4{\cdot}3H_2O$ in air, the temperature range of 25–1000°C, the heating rate of 5°C min^{-1}, the air flow of 50 mL min^{-1}

The complex compound decomposition both in air and nitrogen flow, starts in the range of 25–180°C with an endothermal mass loss of about 4.9 and 5.0%, respectively, which corresponds to 3 molecules of crystallization water. The melting process occurred in course of ligand heating has not been observed. Between 180–210°C, an exothermal peak with maximum at 182°C on DTA curves, in air and nitrogen, can be assigned to a change in crystallization state as no mass modification was observed. A complex decomposition process occurred in air within the temperature range of 180–475°C. The corresponding mass loss was of 42.5% in air, equivalent to $4Cl+4C_6H_5+4(–CH_2–)+(>N–CH_2–CH_2–N<)$ loss and the 4O inserting in the left ligand, the same as for the $Ni_2(C_{50}H_{56}N_{10}O_4)Cl_4$ thermal decomposition [17].

---

[*] Author for correspondence: emosoarca@yahoo.com

1388–6150/$20.00

Akadémiai Kiadó, Budapest, Hungary
Springer, Dordrecht, The Netherlands

Table 1 The thermal decomposition data for $Cu_2(TAMEN)Cl_4 \cdot 3H_2O$ in air and nitrogen atmosphere

Air, *x*=11			Nitrogen, *x*=9			
Temp. range/ °C	Mass loss/%		Temp. range/ °C	Mass loss/%		Mass losses assignments
	Calc.	Found		Calc.	Found	
25–180	4.6	4.9	25–180	4.6	5.0	crystallization water
180–475	47.7	42.3[1]	180–370	47.6	47.7	chlor, phenyl groups, bridge $–CH_2–$, $>N–(CH_2)_2–N<$
475–1000	37.2	40.0[2]	370–1000	37.2	18.2[4]	2,3-dimethyl-5-pyrazolone
Total loss	89.5	87.2[3]	Total loss	89.4	70.9[4]	–
Solid residue	13.4 CuO	13.3 CuO	Solid residue	10.7 Cu	28.9 (10.7 Cu+18.2 l.r.)	–

[1] the difference with reference to calc. mass loss corresponds to 4O(~5.4 mass %) that was inserted by the ligand as partial oxidation process result and that causes the decrease of the found mass to 42.5%

[2] the difference with reference to calc. mass loss corresponds to the content of: –4O≈5.4 mass% from partial oxidation compounds; –2.7% O of CuO (found mass=37.2+5.4–2.7=40)

[3] the difference with reference to calc. mass loss corresponds to the 2.7% O of CuO that causes the decrease of the found mass (89.5–2.7=86.8) and the slight higher quantity of crystallization water

[4] the difference with reference to calc. mass loss corresponds to 18.2% of the ligand rest

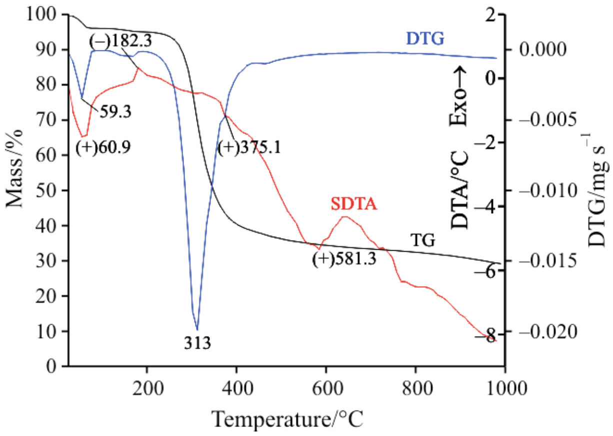

Fig. 2 The thermal decomposition curves of $Cu_2(TAMEN)Cl_4 \cdot 3H_2O$, in nitrogen, the temperature range of 25–1000°C, the heating rate of 5°C min^{-1}, the nitrogen flow of 50 mL min^{-1}

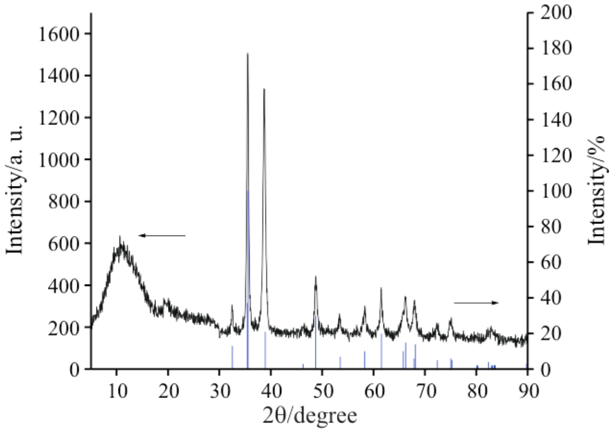

Fig. 3a X-ray diffractogram of solid residue resulted from the thermal decomposition of the $Cu_2(TAMEN)Cl_4 \cdot 3H_2O$ in the temperature range of 25–1000°C with a heating rate of 5°C min^{-1}, in air flow of 50 mL min^{-1} (above); ASTM sheet no. 48–1548 CuO (below)

In the FTIR spectra of ligand heated isothermally to the 400°C for 2 h, only specific bands of pyrazolone were observed. The next step of thermal decomposition in air occurred in the temperature range of 475–1000°C with a mass loss of 40% and it was accompanied by a strong exothermal effect as a result of fast oxidation processes. A solid residue consisting of CuO+ $0.5Cu_2O$ mixture was obtained. Finally, over 800°C, the Cu_2O was oxidized to CuO and, as a result, the mass of solid residue has increased with about 0.5%. This assumption was confirmed of the X-ray pattern of solid residue that exhibits only the specific lines for CuO according to ASTM sheet no. 48–1548 CuO (Fig. 3a).

The thermal decomposition in nitrogen flow, after the crystallization water loss, has occurred by overlapping of ligands degradation processes and their release within the temperature range of 180–370°C with mass loss of 47.7% corresponding to the 4Cl and the $4C_6H_5$+4(–CH_2–)+ (>N–CH_2–CH_2–N<). The last step of decomposition within the temperature range of 370–1000°C was accompanied by about 18.2% mass loss and a solid residue of 28.9% (10.7% for Cu and 18.2% for an organic undefined deposit). The copper was put in evidence by X-ray analysis as it can be seen in Fig. 3b.

The sum of 18.2% of mass loss and 18.2% for organic undefined deposit corresponds to 2,3-dimethyl-5-pyrazolone group mass. In brief, the next scheme of thermal decomposition for $Cu_2(C_{50}H_{56}N_{10}O_4)Cl_4 \cdot 3H_2O$ was proposed:

A) In flow of air

$$\mathrm{Cu_2(C_{50}H_{56}N_{10}O_4)Cl_4{\cdot}3H_2O} \xrightarrow{25\text{–}180^\circ\mathrm{C},\ -3\mathrm{H_2O}}$$
$$\mathrm{Cu_2(C_{50}H_{56}N_{10}O_4)Cl_4} \longrightarrow$$
$$\xrightarrow{180\text{–}475^\circ\mathrm{C},\ -2\mathrm{Cl_2},\ -4\mathrm{C_6H_5},\ -6\mathrm{CH_2},\ -\mathrm{N_2},\ +2\mathrm{O_2}} \mathrm{Cu_2(C_{20}H_{24}N_8O_8)}$$
$$\xrightarrow{475\text{–}800^\circ\mathrm{C},\ -(\mathrm{C_{20}H_{24}N_8O_8}),\ +n\mathrm{O_2}}$$
$$\text{Solid residue (12.8\% mixture of } \mathrm{CuO{:}Cu_2O}=1{:}0.5)$$
$$\xrightarrow{800\text{–}1000^\circ\mathrm{C},\ +0.25\mathrm{O_2}} \text{Solid residue (13.3\% CuO)}$$

B) In flow of nitrogen

$$\mathrm{Cu_2(C_{50}H_{56}N_{10}O_4)Cl_4{\cdot}3H_2O} \xrightarrow{25\text{–}180^\circ\mathrm{C},\ -3\mathrm{H_2O}}$$
$$\mathrm{Cu_2(C_{50}H_{56}N_{10}O_4)Cl_4} \xrightarrow{180\text{–}370^\circ\mathrm{C},\ -2\mathrm{Cl_2},\ -4\mathrm{C_6H_5},\ -3\mathrm{C_2H_4},\ -\mathrm{N_2}}$$
$$\mathrm{Cu_2(C_{20}H_{24}N_8O_4)} \xrightarrow{370\text{–}1000^\circ\mathrm{C},\ -0.5(\mathrm{C_{20}H_{24}N_8O_4})}$$
$$\text{Solid residue 28.9\% (it consists of Cu=10.7\%}$$
$$\text{and } 0.5(\mathrm{C_{20}H_{24}N_8O_4})=18.2\%)$$

The thermal decomposition curves for the $Co_2(TAMEN)Cl_4{\cdot}H_2O$ in air and nitrogen dynamic atmosphere can be seen in Figs 4 and 5.

The thermal decomposition data for $Co_2(TAMEN)Cl_4{\cdot}H_2O$ are given in Table 2.

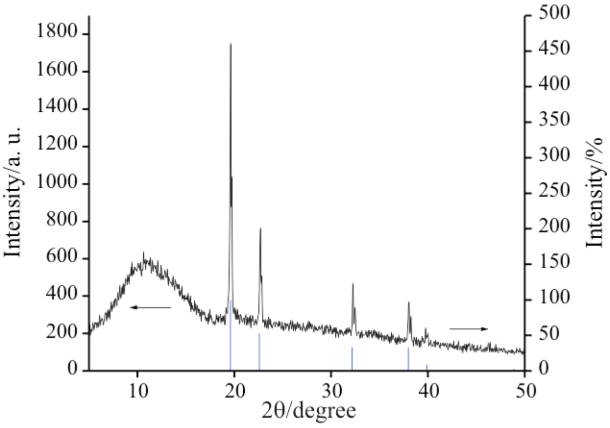

Fig. 3b X-ray diffractogram of solid residue resulted from the thermal decomposition of the $Cu_2(TAMEN)Cl_4{\cdot}3H_2O$ in the temperature range of 25–1000°C with a heating rate of 5°C min^{-1}, in nitrogen flow of 50 mL min^{-1} (above); ASTM sheet no. 01-1241Cu (below)

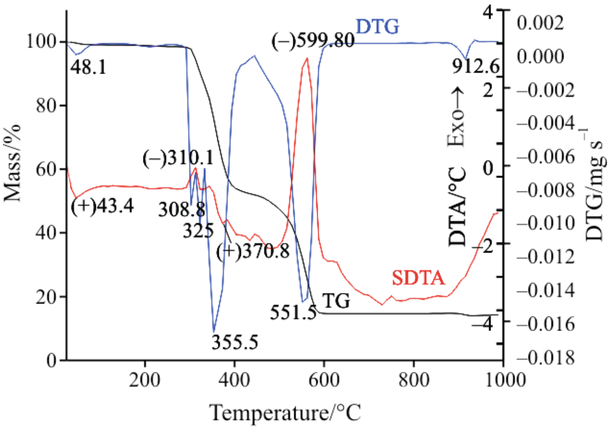

Fig. 4 The thermal decomposition curves of $Co_2(TAMEN)Cl_4{\cdot}H_2O$ in air, the temperature range of 25–1000°C, the heating rate of 5°C min^{-1}, the air flow of 50 mL min^{-1}

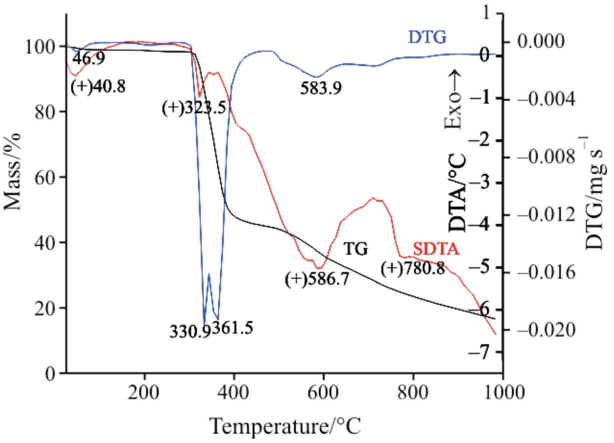

Fig. 5 The thermal decomposition curves of $Co_2(TAMEN)Cl_4{\cdot}H_2O$, in nitrogen, the temperature range of 25–1000°C, the heating rate of 5°C min^{-1}, the nitrogen flow of 50 mL min^{-1}

On both TG curves (air and nitrogen) of the complex compound decomposition, in the range 25–250°C the DTA curves indicate an endothermal process with maxima at 41–43°C. The mass loss for this process is about 1.5–1.7%, the same in air and in nitrogen and this corresponds to loss of one molecule of crystallization water. The melting process occurred in course of the TAMEN ligand heating has not observed. In the FTIR spectra of ligand heated isothermally to the 200°C for 2 h all ligand bands were exhibited.

A complex decomposition process occurred in air within the temperature range of 250–450°C. First, a mass loss of about 12.5%, equivalent with the release of 4Cl, in two steps, was observed on the TG and DTG curves. In the temperature range of 340–450°C the mass loss was of 31.6% in air, equivalent to $4C_6H_5$+4(–CH_2–)+(>N–CH_2–CH_2–N<) mass and the 4O inserting in the left ligand were occurred. They are accompanied of two thermal effects on DTA curves, an exothermal one with maximum at 310°C and an overlapped endothermal, the other one, with two shoulders at 360 and 434°C. The exothermal process with maximum at 310°C can be assigned to an oxidation process in connection with oxygen acquisition.

In the FTIR spectra of ligand heated isothermally to the 400°C for 2 h only specific bands of pyrazolone were observed, what confirms the proper assigning of mass losses to mentioned decomposition processes.

The next step of thermal decomposition in air occurred in the temperature range of 440–800°C with a mass loss of 40.5% that was accompanied with a strong exothermal effect resulted of fast oxidation processes and that corresponds to 2,3-dimethyl-5-pyrazolone group mass. As result, a solid residue consists of a mixture of CoO and Co_3O_4 was obtained.

Table 2 The main thermal decomposition data for $Co_2(TAMEN)Cl_4 \cdot H_2O$ in air and nitrogen atmosphere

Air, *x*=1			Nitrogen, *x*=1			
Temp. range/ °C	Mass loss/%		Temp. range/ °C	Mass loss/%		Mass losses assignments
	Calc.	Found		Calc.	Found	
25–250	1.6	1.5	25–250	1.6	1.7	crystallization water
275–310	12.4	12.5	2500–340	12.4	12.5	chlor
340–450	37.1	31.6[1]	340–400	37.1	37.2	phenyl groups, bridge $–CH_2–$, $>N–(CH_2)_2–N<$
450–800 800–1000	38.6	405[2] 0.7	400–1000	38.5	32.3[4]	2,3-dimethyl-5-pyrazolone, oxygen (in air)
Total loss	89.7	86.8[3]	Total loss	89.6	83.7[4]	–
Solid residue	13.1 CoO	13.2 CoO	Solid residue	10.3 Co	16.3 (10.3 Co+6.0 l.r.)	–

[1] the difference with reference to calc. mass loss corresponds to 4O(~5.6 mass%) that was inserted by the ligand as partial oxidation process result and that causes the decrease of the found mass to 31.6 %

[2] the difference with reference to calc. mass loss corresponds to the content of 4O≈5.6 mass% from partial oxidation compounds and to the 3.7% O of $2/3Co_3O_4$ (found mass=38.6+5.6–3.7=40.5)

[3] the difference with reference to calc. mass loss corresponds to the 2.8% O of CoO and that causes the decrease of the found mass (89.7–2.8=86.9)

[4] the difference with reference to calc. mass loss corresponds to 6.0% of the ligand rest

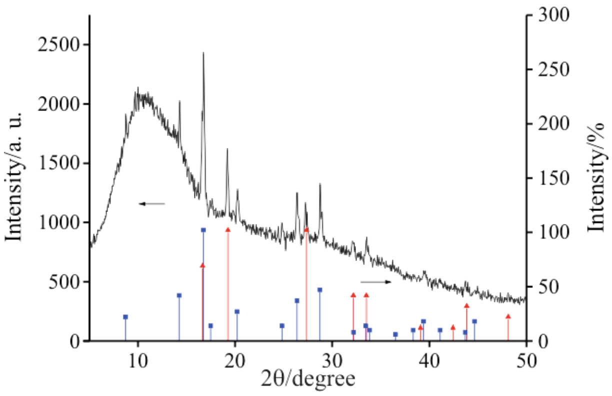

Fig. 6a X-ray diffractogram of solid residue resulted from the thermal decomposition of the $Co_2(TAMEN)Cl_4 \cdot H_2O$ in the temperature range of 25–1000°C with a heating rate of 5° $\cdot min^{-1}$, in air flow of 50 mL min^{-1} (above); ■ – ASTM sheet no. 01-1227 CoO, ▲ – ASTM sheet no. 09-0418(D) Co_3O_4

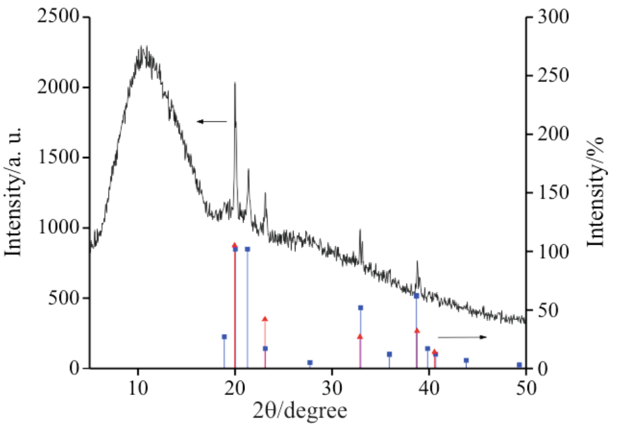

Fig. 6b X-ray diffractogram of solid residue resulted from the thermal decomposition of the $Co_2(TAMEN)Cl_4 \cdot H_2O$ in the temperature range of 25–1000°C with a heating rate of 5°C min^{-1}, in nitrogen flow of 50 mL min^{-1}); ■ – ASTM sheet no. 01-254 Co, ▲ – ASTM sheet no. 15-0806 Co

The last decomposition process pointed out of TG and DTG curves is accompanied with a mass loss of 0.7% with maximum rate at 912.6°C. This can be ascribed to Co_3O_4 decomposition to CoO at 900/950°C [18].

Finally a mixture of CoO and a small quantity of Co_3O_4 (see X-ray diffraction spectrum of Fig. 6a) was obtained.

In nitrogen, the thermal decomposition, after the crystallization water loss, has occurred in three steps:

- The first step within the temperature range of 250–340°C with 12.5% mass loss corresponding to the 4Cl release;
- The second step within the temperature range of 340–400°C with about 37.2% mass loss that corresponds to $4C_6H_5+4(–CH_2–)+(–N–CH_2–CH_2–N–)$ mass;
- The third step within the temperature range of 400–1000°C accompanied of about 32.4% mass loss. The final decomposition result was a solid residue of 16.3% (it consists of 10.3% of Co and 6% for an organic undefined deposit) that was pointed out of Fig. 6b (X-ray spectrum). The sum of 32.4% mass loss and 6.2% for undefined deposit corresponds to 2,3-dimethyl-5-pyrazolone group mass.

In brief, the next scheme of thermal decomposition for $Co_2(C_{50}H_{56}N_{10}O_4)Cl_4 \cdot H_2O$ was proposed:

A) In flow of air

$$Co_2(C_{50}H_{56}N_{10}O_4)Cl_4 \cdot H_2O \xrightarrow{25\text{–}250℃,\ -H_2O}$$
$$Co_2(C_{50}H_{56}N_{10}O)Cl_4 \xrightarrow{250\text{–}340℃,\ -4Cl}$$
$$Co_2(C_{50}H_{56}N_{10}O_4) \xrightarrow{340\text{–}440℃,\ -4C_6H_5,\ -6CH_2,\ -N_2}$$
$$Co_2(C_{20}H_{24}N_8O_4) \xrightarrow{440\text{–}800℃,\ -(C_{20}H_{24}N_8O_4)+nO_2}$$
$$\text{Solid residue (14.0\% } Co_3O_4) \xrightarrow{800\text{–}1000℃,\ -0.25O_2}$$
$$\text{Solid residue (13.2\% CoO)}$$

B) In flow of nitrogen

$$Co_2(C_{50}H_{56}N_{10}O_4)Cl_4 \cdot H_2O \xrightarrow{25\text{–}250℃,\ -H_2O}$$
$$Co_2(C_{50}H_{56}N_{10}O_4)Cl_4 \xrightarrow{250\text{–}340℃,\ -4Cl}$$
$$Co_2(C_{50}H_{56}N_{10}O_4) \xrightarrow{340\text{–}400℃,\ -4C_6H_5,\ -3C_2H_2,\ -N_2}$$
$$Co_2(C_{20}H_{24}N_8O_4) \xrightarrow{400\text{–}1000℃,\ -0.82(C_{20}H_{24}N_8O_4)}$$
$$\text{Solid residue (16.3\% containing Co=10.3\%}$$
$$\text{and } 0.18(C_{20}H_{24}N_8O_4)\text{=6\%)}$$

Conclusions

The $Cu_2(C_{50}H_{56}N_{10}O_4)Cl_4 \cdot 3H_2O$ contains 3 molecules of crystallization water and $Co_2(C_{50}H_{56}N_{10}O_4)Cl_4 \cdot H_2O$ contains one molecule of crystallization water, in air and in nitrogen. Both complex compounds loose their crystallization water under 180°C.

On the whole, the $Cu_2(C_{50}H_{56}N_{10}O_4)Cl_4 \cdot 3H_2O$ and $Co_2(C_{50}H_{56}N_{10}O_4)Cl_4 \cdot H_2O$ thermal decompositions, are similar in air and nitrogen and near to the $Ni_2(C_{50}H_{56}N_{10}O_4)Cl_4 \cdot 8\text{–}9.5H_2O$ thermal decomposition [17]: – the Cl release: – the loss of phenyl group followed of the loss of the $>N\text{–}CH_2\text{–}CH_2\text{–}N<$ group and the bridge $\text{–}CH_2\text{–}$ group; – the degradation of 2,3-dimethyl-5-pyrazolone group and its partial release in nitrogen atmosphere, respectively its burning in air. In air the ligands were completely burned and corresponding oxides were arised from these complex compounds.

The main differences between thermal behavior of compounds in air are:

- In case of $Co_2(C_{50}H_{56}N_{10}O_4)Cl_4 \cdot H_2O$ the decomposition begin at higher temperature, about 290°C, than for the $Cu_2(C_{50}H_{56}N_{10}O_4)Cl_4 \cdot 3H_2O$ and $Ni_2(C_{50}H_{56}N_{10}O_4)Cl_4 \cdot 8\text{–}9.5H_2O$, about 220°C;
- The higher temperature for decomposition beginning of the 2,3-dimethyl-5-pyrazolone group of Co(II) and Cu(II) complex compounds, about 440, respectively 475°C, in comparison with about 340°C for TAMEN as result of cation stabilizing effect by the bonds with two oxygen atoms belonging to antipyrine;
- The higher temperature for the end of decomposition for the 2,3-dimethyl-5-pyrazolone group of $Cu_2(C_{50}H_{56}N_{10}O_4)Cl_4 \cdot 3H_2O$, about 680°C, in comparison with about 600°C for $Co_2(C_{50}H_{56}N_{10}O_4)Cl_4 \cdot H_2O$ and about 580°C for $Ni_2(C_{50}H_{56}N_{10}O_4)Cl_4 \cdot 8\text{–}9.5H_2O$, that means the stronger stabilizing effect on the 2,3-dimethyl-5-pyrazolone group of ligand for Cu(II) cation;

The results in nitrogen confirm the higher temperature of decomposition begin for $Co_2(C_{50}H_{56}N_{10}O_4)Cl_4 \cdot H_2O$ and the stronger stabilizing effect on the 2,3-dimethyl-5-pyrazolone group of ligand for Cu(II) cation.

In air, the ligands were completely decomposed to volatile compounds and as result of thermal decomposition a solid residue of CuO, respectively CoO, was obtained. In nitrogen, some solid deposit was arised from complex compounds consist of organic deposit of ligand and metallic Cu or Co.

References

1 T. Rosu, S. Pasculescu, V. Lazar, C. Chifiriuc and R. Cernat, Molecules, 11 (2006) 904.
2 R. K. Agarwal and S. Prasad, Bioinorg. Chem. Appl., 3 (2005) 3.
3 K. Z. Ismail, A. El-Dissouky and A. Z. Shehada, Polyhedron, 16 (1997) 2909.
4 R. K. Agarwal, L. Singh and D. Kumar Sharma, Bioinorg, Chem. Appl., 1 (2006) 1.
5 N. Kalarani, S. Sangeetha, P. Kamalakannan and D. Venkappayya, Russ. J. Coord. Chem., 29 (2003) 909.
6 O. Costisor, W. Linert, S. Deutsch and C. Stanescu, J. Coord. Chem., 33 (1994) 229.
7 R. Tudose, I. Pantenburg, E. M. Mosoarca, G. Meyer and O. Costisor, Z. Anorg. Allg. Chem., 632 (2006) 1491.
8 R. Tudose, I. Pantenburg, E. M. Mosoarca, G. Meyer and O. Costisor, Z. Anorg. Allg. Chem., 631 (2005) 2423.
9 R. Alexandrova, G. Rashkova, T. Popova, R. Tudose, E. M. Mosoarca, S. Slavov and O. Costisor, Acta Morph. Anthrop., 11 (2006) 60.
10 R. Alexandrova, G. Rashkova, T. Popova, R. Tudose, E. M. Mosoarca, S. Slavov and O. Costisor, Exp. Path. Parasit., 8/2 (2005) 93.
11 R. Alexandrova, A.Vacheva, M. Kirilova, G. Miloshev, E.M. Mosoarca, R. Tudose and O. Costisor, Acta. Morphol. Anthropol., 12 (2007) 72.
12 W. Linert, O. Costisor and R. Tudose, Orient. J. Chem., 11 (1995) 107.
13 O. Costisor, R. Tudose, I. Pantenburg and G. Meyer, Z. Naturforsch., 57B (2002) 1454.
14 I. Labadi, R. Tudose, I. Fejer, Z. Jori and O. Costisor, J. Therm. Anal. Cal., 56 (1999) 553.
15 I. Labadi, Zs. Czibulya, R. Tudose and O. Costisor, J. Therm. Anal. Cal., 77 (2004) 553.
16 I. Labadi, E. Pal, R. Tudose and O. Costisor, J. Therm. Anal. Cal., 83 (2006) 681.
17 V. Sasca, E. M. Mosoarca, L. Avram, R. Tudose and O. Costisor, J. Therm. Anal. Cal., DOI: 10.1007/s10973-008-9106-z.
18 IUCLID Dataset, tricobalt tetraoxide, 1308-06-1/18 Febr. 2000, p. 8.

DOI: 10.1007/s10973-008-9107-y